Biochimica et Biophysica Acta 1818 (2012) 55–63

Contents lists available at SciVerse ScienceDirect

Biochimica et Biophysica Acta

journal homepage: www.elsevier.com/locate/bbamem

Electrostatic interaction between inactivation ball and T1–S1 linker region of Kv1.4 channel

Zhuo Fan, Xuying Ji, Mingyu Fu, Wanming Zhang, Du Zhang, Zhongju Xiao *

Department of Physiology, School of Basic Medical Sciences, Southern Medical University, Guangzhou 510515, China

ARTICLE INFO

Article history:
Received 3 May 2011
Received in revised form 26 September 2011
Accepted 26 September 2011
Available online 4 October 2011

Keywords:
Kv1.4 channel
Inactivation
"Ball and chain" model
Electrostatic interaction

ABSTRACT

Inactivation of potassium channels plays an important role in shaping the electrical signaling properties of nerve and muscle cells. The rapid inactivation of Kv1.4 has been assumed to be controlled by a "ball and chain" inactivation mechanism. Besides hydrophobic interaction between inactivation ball and the channel's inner pore, the electrostatic interaction has also been proved to participate in the "ball and chain" inactivation process of Kv1.4 channel. Based on the crystal structure of Kv1.2 channel, the acidic T1–S1 linker is indicated to be a candidate interacting with the positively charged hydrophilic region of the inactivation domain. In this study, through mutating the charged residues to amino acids of opposite polar, we identified the electrostatic interaction between the inactivation ball and the T1–S1 linker region of Kv1.4 channel. Inserting negatively charged peptide at the amino terminal of Kv1.4 channel further confirmed the electrostatic interaction between the two regions.

1. Introduction

A-type current of potassium ion channels plays an important role in shaping the action potential and modulating the firing frequency of excitable cells [1]. Among the A-type channels, the *Drosophila Shaker* K^+ channel (ShB) has been most extensively studied. This kind of channel is characterized by its rapid inactivation after short opening to depolarized membrane potential. The rapid inactivation mechanism of ShB channel belongs to the typical N-type inactivation (also called "ball and chain" inactivation) [2,3], which is first proposed by Armstrong and Bezanilla in studying the inactivation mechanism of voltage-gated Na^+ channel [4–6]. In this model, a positively charged N-terminal inactivation ball, tethered by a hydrophilic chain, inactivates a channel by diffusing into the channel pore and occludes it shortly after its opening (Fig. 1). It has been proposed that 20 amino acids on the NH_2-terminal of ShB constitute the inactivation domain of ShB, of which the first 11 hydrophobic residues play roles in inactivation by interacting with the hydrophobic wall of the inner pore [2,7–9]. The subsequent 9 hydrophilic residues of inactivation domain, carrying 2 net positive charges, play an important role in speeding the diffusion rate of the inactivation domain toward its binding site through long-range electrostatic interaction [2,10–12].

Some mammalian voltage-gate potassium ion channels, like Kv1.4, Kv3.3, Kv3.4 and Kv4.2, also exhibit N-type inactivation [13–17]. Similar to ShB, the time course of rapid inactivation of Kv1.4 channel is determined by both hydrophobic and electrostatic interactions [13,18–20]. The first 37 amino acids constitute the inactivation ball of Kv1.4, which comprises an NH_2-terminal hydrophobic region and a COOH-terminal hydrophilic region. The hydrophilic region (residues 26–37), carrying 3 net positive charges, is thought to facilitate the inactivation process of Kv1.4 via electrostatic interactions [13]. The crystal structure of the mammalian *Shaker* family Kv channel showed that 4 linkers connecting the tetrameric T1 domains and the transmembrane S1 domains form 4 large side portals [21,22]. In contrast to the narrow and positively charged center hole of T1 assembly, which is hardly to allow K^+ passing through, the T1–S1 side portals are large enough to allow K^+ ions, organic pore-blocking cations, and even the inactivation peptides to flow freely between the cytoplasm and the transmembrane pore. The presence of the multiple negative charges on the surface of the side portal makes it a good candidate for the site to interact with the positively charged inactivation ball through long-range electrostatic interactions.

In this study, we made a series mutations on regions including the positively charged region of the inactivation ball, the negatively charged T1–S1 linker region and both of them for Kv1.4 channel. These mutations include substituting the positively charged residues of inactivation ball with negatively charge residues, substituting the negatively charged residues of T1–S1 linker with positively charged amino acids, and simultaneously mutating residues of the two regions to residues of opposite polarity (Fig. 2). The different influences of these mutations on the inactivation time course confirmed the electrostatic interactions between the positively charged inactivation ball and the negatively charged T1–S1 linker. In addition, we inserted a peptide carrying 3 negatively charged residues at different positions

* Corresponding author. Tel./fax: +86 20 61648604.
E-mail address: xiaozj@fimmu.com (Z. Xiao).

0005-2736/$ – see front matter © 2011 Elsevier B.V. All rights reserved.
doi:10.1016/j.bbamem.2011.09.028

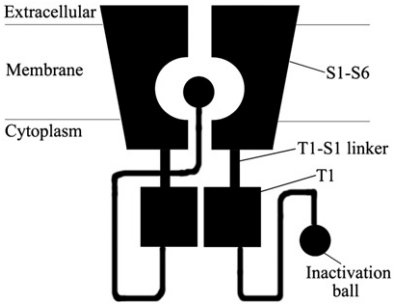

Fig. 1. The "ball and chain" inactivation model of Kv1.4. In this model the inactivation "ball" linked by a "chain" inactivates the channel by interacting with the inner pore. S1–S6, the six transmembrane domains of Kv1.4 channel. T1, the tetramerization domain responsible for the subfamily specificity of channel assembly.

of NH_2-terminal of Kv1.4. We found that, the mutants inactivated more and more slowly with the insertion site moving nearer to the extreme NH_2-terminal. These results further confirmed the long-range electrostatic interactions in the inactivation process of Kv1.4 channel.

2. Materials and methods

2.1. Molecular biology

Fig. 2 shows the amino-terminal sequences of Kv1.4 and the mutants investigated in this study. $Kv1.4_{R-E}$ was constructed by mutating arginine (R) of 26,28,30,32 into glutamine (E) simultaneously. Similarly, $Kv1.4_{E-R}$ was constructed by mutating E 279, E 280, E 281 and D 282 into opposite charged arginine (R). When both of the 2 regions were mutated in the same way above in one mutant, we named it $Kv1.4_{both}$. $Kv1.4_{insert1}$, $Kv1.4_{insert2}$ and $Kv1.4_{insert3}$ mean inserting negatively charged peptide of SGDEDSG after positions 19, 39 and 50 respectively. All these 3 inserting sites are in flexible random-coil regions according to the NMR structure of amino terminal of Kv1.4 channel [23]. All of the mutants were generated by overlap PCR. For $Kv1.4_{R-E}$ and $Kv1.4_{E-R}$, 4 primers were used in the first round PCR to obtain two fragments (fragment I and fragment II). The sense primer for fragment I, containing the *EcoR*I site and ATG start coden, is corresponding to the sequence near the 5′ end of Kv1.4WT. The anti-sense primer for fragment II is complementary to the 3′ end of Kv1.4WT and contains *BamH*I site and TAA stop coden. The anti-sense primer of fragment I and sense primer of fragment II containing the mutation nucleotides are complementary to the appropriate site and have overlapping sequence with each other. The construction of $Kv1.4_{both}$ was the same with $Kv1.4_{E-R}$, except that the template was $Kv1.4_{R-E}$ rather than Kv1.4WT. For the insertion mutants, the inserting nucleotide sequences were included in the anti-sense primer of fragment I and sense primer of fragment II. After the first round PCR, fragment I and fragment II were ligated together by overlap PCR and the final genes with mutation sequence were obtained. Then, the resulting mutation genes after overlap PCR were cut with *EcoR*I and *BamH*I restriction enzymes(MBI, Ferments, Harrington, Burlington, CANADA) and subcloned into a *pcDNA3* vector cut with the same restriction enzymes. The plasmids containing the mutation genes were finally transformed into DH5α competent cells. After enzymatic or PCR identification, all the mutants were confirmed by sequencing to ensure the absence of errors.

2.2. Cell culture

CHO-K1 cells were grown in Ham's F-12 nutrient mixture (Invitrogen, Co. Grand Island, N.Y.) supplemented with 10% fetal bovine serum, in a humidified 37 °C incubator (5% CO_2). The cells were passaged twice weekly through exposure to 0.05% trypsin, diluted in 0.5 mM EDTA in PBS. For gene transfection, the cells were transferred to poly-L-lysine coated glass coverslips. After cell density reached 50–70% confluence, rKv1.4WT or its mutant genes was transiently co-expressed with pEGFP (Clontech, Palo Alto, CA) using LipofectAMINE Plus(TM) reagent (Invitrogen). Cells showing GFP fluorescence were chosen after 24 h of transfection for use in electrophysiological experiments.

2.3. Electrophysiology

Standard whole cell voltage-clamp recordings were performed by using a MultiClamp 700B amplifier (Axon Instruments, Union City, CA) and digitized through a Digidata 1332A interface (Axon Instruments, Union City, CA) at room temperature. Currents were low pass filtered at 2 kHz and sampled at 10 kHz. Pipettes were pulled from borosilicate glass and had a resistance of between 2 and 4 MΩ. The pipette solution was (in mM): 140 KCl, 10 EGTA, 1 $CaCl_2$, 2 Mg-ATP and 10 HEPES (pH 7.2, with KOH). For high intracellular Mg^{2+} concentration ($[Mg^{2+}]_i$), the Mg^{2+} concentration of the pipette solution was increased to 20 mM, while 10 mM KCl and 10 mM EGTA were removed to keep the osmolarity unchanged. The extracellular solution was Hanks' balanced salts solution (HBSS, Sigma; in mM): 1.3 $CaCl_2$, 0.8 $MgSO_4$, 5.4 KCl, 0.4 KH_2PO_4, 136.9 NaCl, 0.3 Na_2HPO_4,

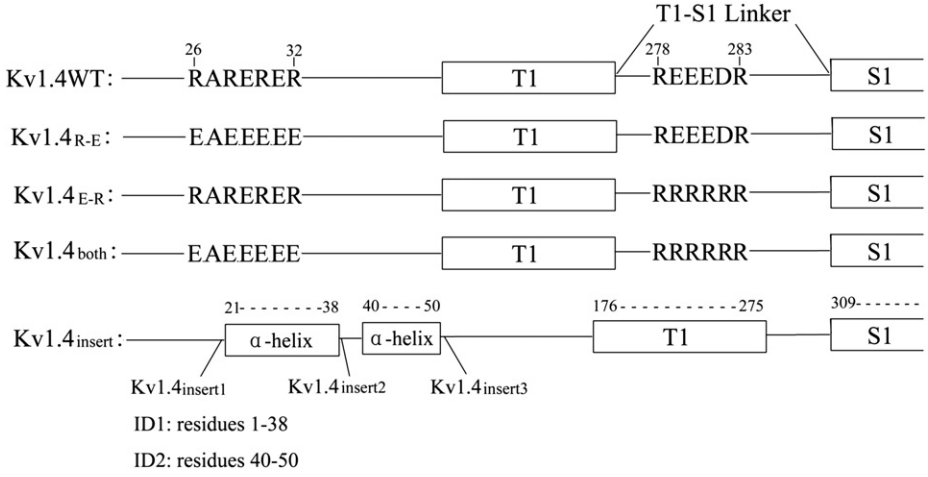

Fig. 2. Schematic representations of the wild type and mutant Kv1.4 channels. The positively charged amino acids of inactivation domain and negatively charged amino acids of T1–S1 liker region are shown on the top. The constructs mutating on positive charges, negative charges or both are shown below. The mutants by inserting negatively charged peptide at different positions are shown at the bottom and the α-helices constituted by residues 21–38 of ID1 and residues 40–50 of ID2 are indicated. The inserting peptide containing 3 negative charges was SGDEDSG.

10 D-glucose and 4.2 $NaHCO_3$. 80% compensation of the series resistance was used for currents exceeding 2 nA. Holding potential was maintained at −90 mV. To obtain activation curves, the currents were evoked by step depolarization to test potentials between −90 and +70 mV for 500 ms in 20 mV increments. Steady-state inactivation curves were obtained using a standard two-step protocol, which involved a pre-pulse of 1 or 5 s at potentials between −90 and +50 mV (10-mV increments) and a test pulse of +30 mV to determine the fraction of channels inactivated during the pre-pulse. The recovery course from inactivation was measured with a standard two-pulse protocol. A P1 pulse to +30 mV was applied for 2 s, then cells were repolarized with a recovery potential of −100 mV for a variable duration (200 ms to 41 s) before stepping back to a 500 ms test potential (P2) of +30 mV. Data were acquired with the pClamp10 software (Axon Instruments) and further analyzed using clampfit (Axon Instruments) and Origin 7.0 (OriginLab, Northampton, MA). All of the data are shown as means ± S.E.M. Statistical analysis was carried out by one-way ANOVA using a Bonferroni test. The criterion for a significant difference was $p<0.05$.

3. Results

3.1. Effect of substituting the negatively charged amino acids on T1–S1 linker by positively charged arginine (R)

To investigate the effect of negative charges of T1–S1 linker on inactivation, we mutated 4 negatively charged amino acids (from E 279 to D 282) simultaneously to positively charged arginine (R). The macroscopic current traces of Kv1.4WT and $Kv1.4_{E-R}$ are shown in Fig. 3A and Fig. 3B respectively. Currents of Kv1.4WT and $Kv1.4_{E-R}$ recorded at +70 mV are normalized and superimposed in Fig. 3C. $Kv1.4_{E-R}$ inactivated more slowly compared with Kv1.4WT. Time constant of inactivation for $Kv1.4_{E-R}$ at +70 mV was 49.8 ± 4.4 ms (n = 9), which was significantly larger than that of Kv1.4WT (26.8 ± 1.4 ms, n = 6, $p<0.01$). Time constants of inactivation (τ_{inact}) for the mutant and Kv1.4WT were plotted against membrane voltage from −10 mV to +70 mV (Fig. 3D). τ_{inact} of $Kv1.4_{E-R}$ were larger than that of Kv1.4WT at each voltage, which suggests that the decelerating effect on inactivation caused by the mutation is not dependent on membrane voltage. The result, that replacing negatively charged residues on T1–S1 liner by amino acids of opposite polar slowed down the inactivation rate, suggests that the negative charges on this region play roles in inactivation of Kv1.4 channel by accelerating the inactivation course.

3.2. Effect of substituting the positively charged amino acids on inactivation domain by negatively charged glutamine (E)

Next, we studied the influence of positive charges of inactivation domain on inactivation of Kv1.4 channel. Similarly, we replaced the positively charged amino acids of 26, 28, 30 and 32 by negatively charged glutamine (E) in a mutant named $Kv1.4_{R-E}$. Fig. 4A and B shows the current traces of Kv1.4WT and $Kv1.4_{R-E}$ respectively. The normalized currents of Kv1.4WT and $Kv1.4_{R-E}$ recorded at +70 mV are superimposed in Fig. 4C to compare the differences in decay time between them. Inactivation of $Kv1.4_{R-E}$ was much slower than that of Kv1.4WT. Time constant of inactivation for $Kv1.4_{R-E}$ at +70 mV was 349.1 ± 35.6 ms (n = 5), which was about 13 times larger than that of Kv1.4WT (26.8 ± 1.4 ms, n = 6, $p<0.00001$). Fig. 4D shows that the decelerating effect caused by the mutation is voltage-independent. The result that $Kv1.4_{R-E}$ inactivated much more slowly than Kv1.4WT suggests that the positive charges of the inactivation domain play an important role in the inactivation process of Kv1.4 channel.

3.3. Effect of mutating charged amino acids of the two regions (inactivation domain and T1–S1 linker) simultaneously

The above experiments have demonstrated that the mutants, with inactivation domain and T1–S1 linker carrying charges of the same

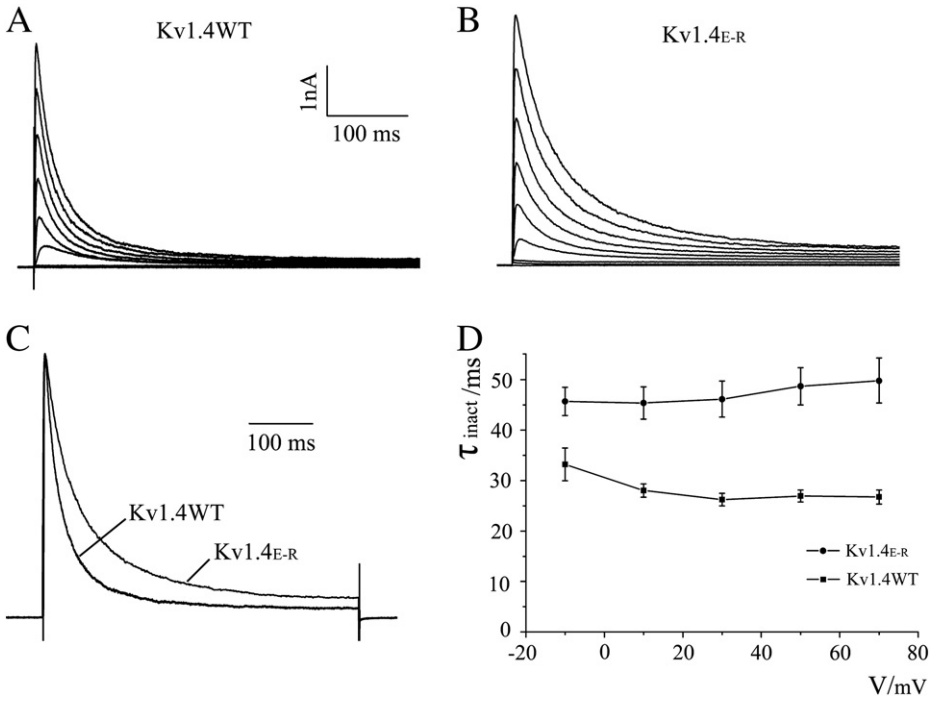

Fig. 3. Effect of substituting the negatively charged amino acids on T1–S1 linker by positively charged arginine (R). (A, B) Representative whole-cell current traces for Kv1.4WT and $Kv1.4_{E-R}$, which were transiently expressed in CHO-K1 cells. (C) Normalized current traces for Kv1.4WT and $Kv1.4_{E-R}$ at +70 mV. (D) Comparison of inactivation time constants (τ_{inact}) for Kv1.4WT and $Kv1.4_{E-R}$ at different membrane voltages (from −10 mV to +70 mV). The currents were evoked by step depolarization to test potentials between −90 and +70 mV for 500 ms in 20 mV increments. Inactivation time constants (τ_{inact}) were obtained using a single exponential function fitted to the decaying period of current traces recorded at +70 mV.

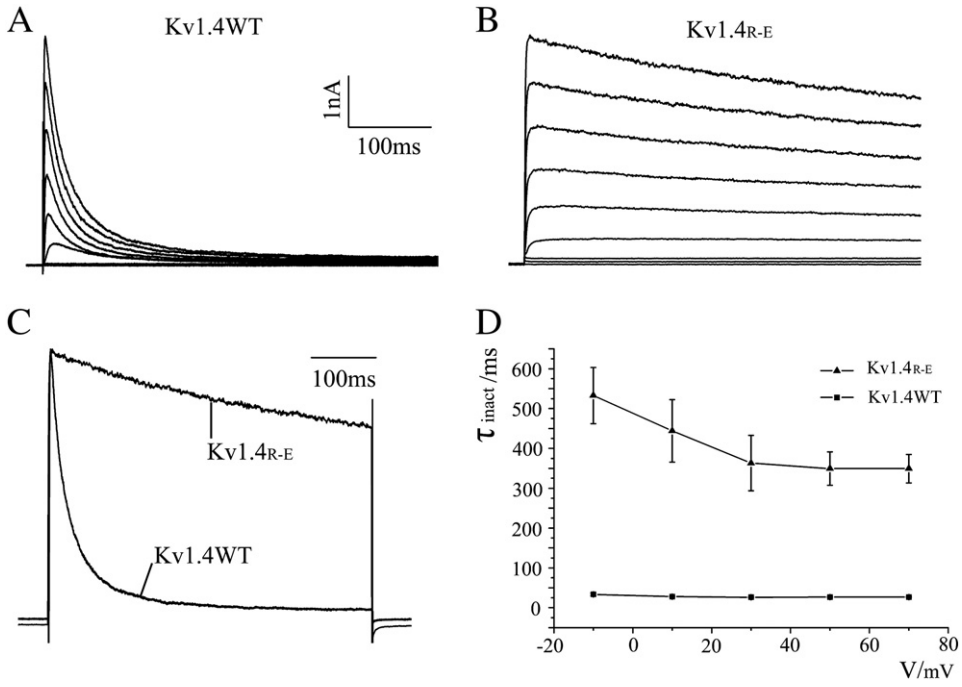

Fig. 4. Effect of substituting the positively charged amino acids on inactivation domain by negatively charged glutamine (E). (A, B) Representative current traces for Kv1.4WT and Kv1.4$_{R-E}$. (C) Normalized current traces for Kv1.4WT and Kv1.4$_{R-E}$ at +70 mV. (D) Comparison of inactivation time constants (τ_{inact}) for Kv1.4WT and Kv1.4$_{R-E}$ at different membrane voltages (from −10 mV to +70 mV).

polarity (both positive for Kv1.4$_{E-R}$ and both negative for Kv1.4$_{R-E}$), inactivated more slowly than Kv1.4WT (with the two regions carrying charges of opposite polarity). To examine the electrostatic interaction between inactivation domain and T1–S1 linker region, it is necessary to mutate the charged amino acids of the two regions simultaneously in one mutant (named Kv1.4$_{both}$). Fig. 5A shows the normalized and superimposed currents recorded at +70 mV of all the mutants and Kv1.4WT. Although Kv1.4$_{both}$ inactivated more

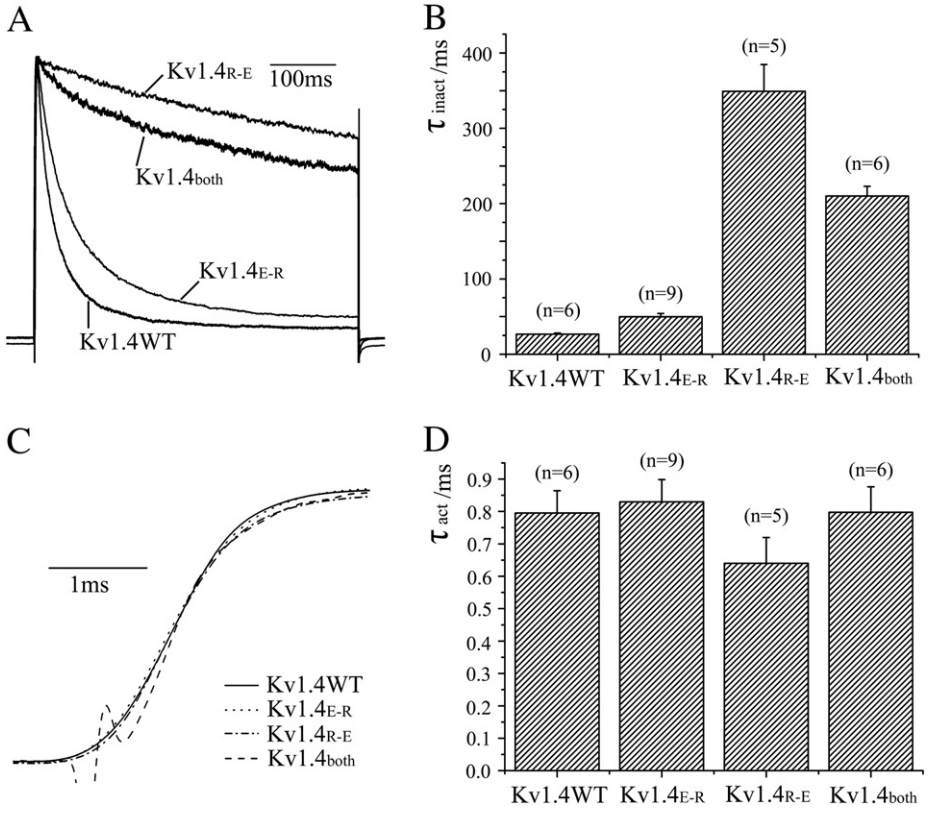

Fig. 5. Effect of mutating charged amino acids of the two regions (inactivation domain and T1–S1 linker) simultaneously. (A) Normalized current traces for Kv1.4$_{both}$, Kv1.4WT, Kv1.4$_{E-R}$ and Kv1.4$_{R-E}$ at +70 mV. (B) Comparison of inactivation time constants for Kv1.4WT, Kv1.4$_{both}$ and the other two mutants (Kv1.4$_{E-R}$ and Kv1.4$_{R-E}$). (C) The growing period of normalized current traces of all the constructs were enlarged and superimposed. (D) The activation time constants (τ_{act}) for Kv1.4WT and the other 3 mutants.

slowly compared with Kv1.4WT ($p<0.00001$), it had an inactivation rate which was significantly faster than $Kv1.4_{R-E}$ ($p<0.01$). The inactivation time constant of $Kv1.4_{both}$ and $Kv1.4_{R-E}$ were 210.0 ± 13.0 ms ($n=6$) and 349.1 ± 35.6 ms ($n=5$), respectively (Fig. 5B). This suggests that there exists long-distance electrostatic interaction between opposite charging residues of inactivation domain and T1–S1 linker region. Moreover, despite the same number of amino acids mutated, $Kv1.4_{R-E}$ slowed the inactivation much more severely compared with $Kv1.4_{E-R}$ (Fig. 5A and B). This result suggests that, compared with the negative charges on T1–S1 linker region, the positive charges of inactivation domain have much more impact on the inactivation of Kv1.4 channel. Considering it, the result that $Kv1.4_{both}$ did not inactivate as rapidly as Kv1.4WT will be not surprising.

3.4. The activation time constant was not changed by mutations

Besides inactivation time constants, we also measured the time constants of activation for mutants and Kv1.4WT by fitting the rising period of current trace at +70 mV with single exponential growing function. Fig. 5C shows that the growing period of normalized current traces for the mutants and Kv1.4WT overlapped each other well. The activation time constants were 0.80 ± 0.07 ms, 0.83 ± 0.07 ms, 0.64 ± 0.08 ms and 0.80 ± 0.08 ms for Kv1.4WT, $Kv1.4_{E-R}$, $Kv1.4_{R-E}$ and $Kv1.4_{both}$ respectively. In contrast to the large differences of inactivation time constants, there were no significantly differences in time constants of activation between the mutants and Kv1.4WT, which suggests that the activation gate was not influenced by these mutations.

3.5. Voltage dependence of steady-state inactivation

Next, we examined if the voltage-dependent properties of steady-state inactivation were altered by these mutations. The voltage-dependence of inactivation was measured by using a standard two-pulse protocol with inactivation pulse (P1) over the range of −90 to +50 mV followed by a test pulse (P2) to +30 mV. Fig. 6A–D shows the currents of Kv1.4WT, $Kv1.4_{E-R}$, $Kv1.4_{R-E}$ and $Kv1.4_{both}$ elicited upon the two-pulse protocol respectively. The current at the test pulse represents channels still available for opening. The steady-state availabilities for the mutants were determined by subtracting the non-inactivated currents measured at the end of the test pulses from the total currents before normalized, thereby analyzing only the inactivated portion of the currents. The normalized peak currents of test pulse are plotted as a function of pre pulse potentials and fitted to Boltzmann function (Fig. 6E). The half-inactivation potential ($V_{1/2}$) of $Kv1.4_{R-E}$, $Kv1.4_{both}$ and $Kv1.4_{E-R}$ were -40.0 ± 1.0 mV ($n=9$), -42.2 ± 0.8 mV ($n=11$) and -48.1 ± 0.9 mV ($n=12$) respectively, all shifting toward the positive direction compared with Kv1.4WT (-53.1 ± 0.7 mV, $n=12$). Among these constructs, $Kv1.4_{R-E}$, which inactivates most slowly, has the largest $V_{1/2}$ whereas Kv1.4WT, which inactivates fastest, has the smallest $V_{1/2}$. The values of $V_{1/2}$ for $Kv1.4_{both}$ and $Kv1.4_{E-R}$ are between them. $Kv1.4_{both}$, which inactivated more slowly compared with $Kv1.4_{E-R}$, has a $V_{1/2}$ shifting rightward by about 6 mV relative to $Kv1.4_{E-R}$. With the inactivation rates of the mutants becoming slower, the half-inactivation potentials of them shift toward positive direction. These results suggest that mutation on charges of hydrophilic region of inactivation domain or T1–S1 linker region not only influenced the inactivation rate but also the voltage dependence of inactivation. We also compared the voltage-dependence of activation for the wild type and mutant channels and obtained no significant differences between them (data are not shown).

3.6. Effect of elevating intracellular Mg^{2+} concentration on inactivation of $Kv1.4_{R-E}$

To further confirm the electrostatic interaction between the inactivation ball and T1–S1 linker region, we examined the charge screening effect of elevating $[Mg^{2+}]_i$ on inactivation of $Kv1.4_{R-E}$, which exhibited the slowest decay rate. The normalized currents at +70 mV for $Kv1.4_{R-E}$ in 2 and 20 mM $[Mg^{2+}]_i$ are superimposed and shown in Fig. 7A. τ_{inact} at +70 mV was 277.7 ± 10.1 ms ($n=9$) in 20 mM $[Mg^{2+}]_i$, which was significantly smaller than that in 2 mM $[Mg^{2+}]_i$ (349.1 ± 35.6 ms, $n=5$, $p<0.05$). Elevating intracellular Mg^{2+} concentration accelerated inactivation rate of $Kv1.4_{R-E}$ by reducing the electrostatic repulsion between the negatively charged inactivation domain and the T1–S1 linker region. The accelerating effect did not exhibit obvious voltage-dependence (Fig. 7B).

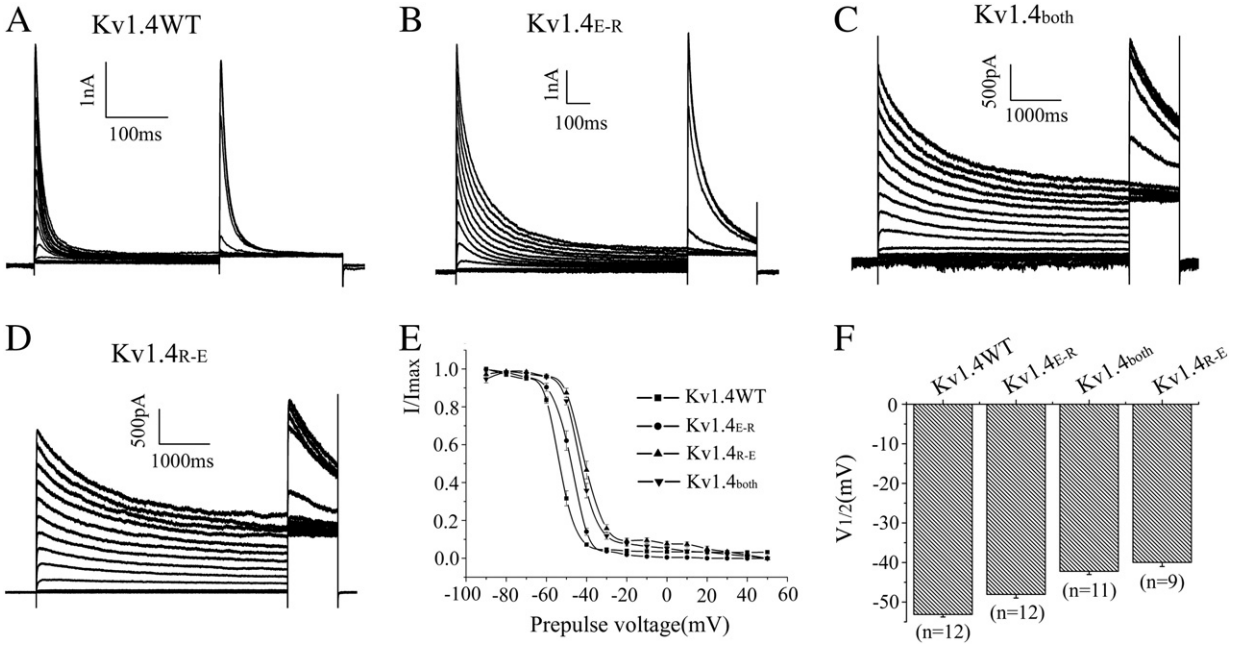

Fig. 6. Voltage-dependence of inactivation. (A–D) Currents elicited upon the two pulse protocol for Kv1.4WT, $Kv1.4_{E-R}$, $Kv1.4_{R-E}$ and $Kv1.4_{both}$ respectively. (E) The normalized peak currents of test pulse as a function of pre pulse potentials. (F) The half inactivation potential ($V_{1/2}$) for Kv1.4WT and the mutants. The steady-state availabilities for the mutants were determined by subtracting the non-inactivating currents measured at the end of the test pulses from the total currents before they are normalized. $V_{1/2}$ was obtained by fitting the voltage-dependent inactivation curve with a Boltzmann function ($I/Imax=1/[1+\exp(V-V_{1/2})/k]$).

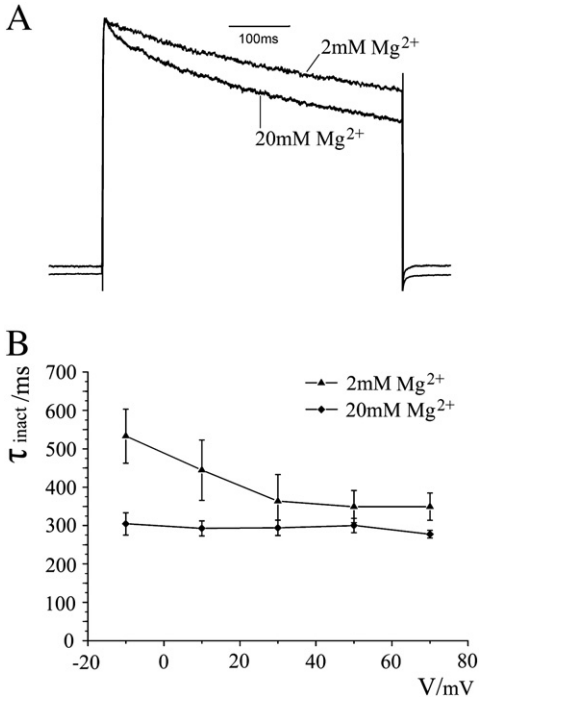

Fig. 7. Effect of elevating $[Mg^{2+}]_i$ on inactivation of $Kv1.4_{R-E}$. (A) Normalized current traces for $Kv1.4_{R-E}$ at +70 mV in 2 mM and 20 mM $[Mg^{2+}]_i$. (B) τ_{inact} for $Kv1.4_{R-E}$ in 2 mM and 20 mM $[Mg^{2+}]_i$ plotted against membrane voltage.

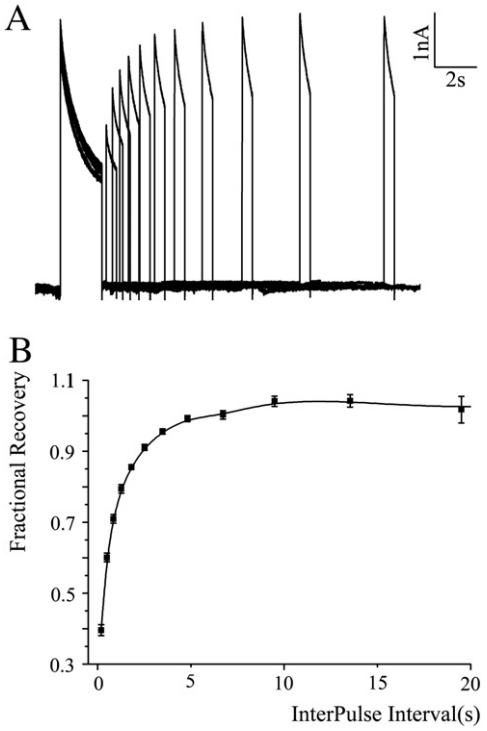

Fig. 8. Recovery from inactivation of $Kv1.4_{R-E}$ mutant channel. (A) Currents of $Kv1.4_{R-E}$ measured using a two pulse protocol. (B) Fractional recovery was plotted as a function of the interpulse interval. The fractional recovery was defined as the ratio of peak values of P1 and P1, both subtracting the non-inactivating component at the end of P1. The fractional recovery curve was fitted to a single exponential function to obtain the time constant of recovery rate (τ_{rec}).

In addition to the result of decelerating the inactivation rate of Kv1.4WT by elevating $[Mg^{2+}]_i$ we have demonstrated previously [24], the charge screening effect of elevating intracellular Mg^{2+} concentration on inactivation of $KV1.4_{R-E}$ confirmed the electrostatic interaction between inactivation ball and T1–S1 linker region.

3.7. Recovery from inactivation of $Kv1.4_{R-E}$ is not changed by mutation

Besides the inactivation properties (including inactivation rate and voltage-dependence of inactivation), we also investigated the time course of dissociation from inactivation for $Kv1.4_{R-E}$. The recovery (dissociation) course from inactivation was measured with a standard two-pulse protocol. Fig. 8A shows an example of raw data traces obtained from $Kv1.4_{R-E}$. To measure the recovery rate, the ratios of peak currents of the P2 and P1, each subtracting the non-inactivating component at the end of P1, were plotted against the inter-pulse interval, and fitted with a single-exponential function (Fig. 8B). The time constant of recovery (τ_{rec}) for $Kv1.4_{R-E}$ was 1272.5 ± 181.3 ms (n = 11), which was not significantly different from that for Kv1.4WT (1337.4 ± 253.8 ms, n = 9) we examined previously. This result suggests that although mutation on inactivation domain largely reduced the inactivation rate, it did not exert any influences on the recovery rate from inactivation.

3.8. Effect of inserting negatively charged peptide in the NH_2-terminal on inactivation of Kv1.4

The above experiments have suggested that the positive charges of inactivation domain and negative charges of T1–S1 linker both facilitate the inactivation process of Kv1.4 channel, although the impact of inactivation domain is more severely. The result of mutating both of the two regions indicated the electrostatic attraction between inactivation ball and T1–S1 linker region. To further identify the role of charges of NH_2-terminal on inactivation, we inserted a small negatively charged peptide (SGDEDSG) at different positions of amino-terminal, and compared the inactivation rates of the mutants with that of Kv1.4WT. We chose Y19, A39 and A50 as the positions after which the charged peptide was inserted. According to the NMR structure of the amino-terminal of Kv1.4, these positions were all in the flexible linker regions [23]. Fig. 9A shows the normalized current traces of the three mutants and Kv1.4WT recorded at +70 mV. The inactivation time constants of $Kv1.4_{insert1}$, $Kv1.4_{insert2}$, $Kv1.4_{insert3}$ and Kv1.4WT were 582.6 ± 71.5 ms (n = 4), 380.4 ± 14.5 ms (n = 5), 216.1 ± 20.6 ms (n = 5) and 26.8 ± 1.4 ms (n = 6) respectively (Fig. 9B). With the insertion site moving toward the extreme amino-terminal, the mutants inactivated more and more slowly. This result can be explained by the electrostatic repulsion between the inserting peptide in amino terminal and the T1–S1 linker region, which further confirmed the role of the electrostatic interaction in inactivation of Kv1.4 channel.

4. Discussion

The "ball and chain" model of inactivation has been demonstrated to be mediated through occluding the channel pore by hydrophobic interaction between the inactivation ball and the inner pore. The inactivation balls of both ShB and Kv1.4 include two regions with different properties — the amino terminal hydrophobic region and the carboxyl terminal hydrophilic region. The hydrophilic region of inactivation ball of either ShB or Kv1.4 has several net positive charges which have been proved to facilitate the inactivation process by accelerating the diffusing rate of inactivation ball toward its binding site. Deleting charged residues of this region or neutralization them slowed macroscopic inactivation of ShB channel induced by inactivation domain or synthetic peptide [2, 25]. For Kv1.4 channel, deletion of the hydrophilic region (residues 26–37) which contains three net positive charges greatly attenuated inactivation [13,26]. All these results suggest that the charges in the hydrophilic region of inactivation domain accelerate the N-type inactivation through electrostatic interaction. The crystal structure of T1 domain of *Shaker* family Kv1.1

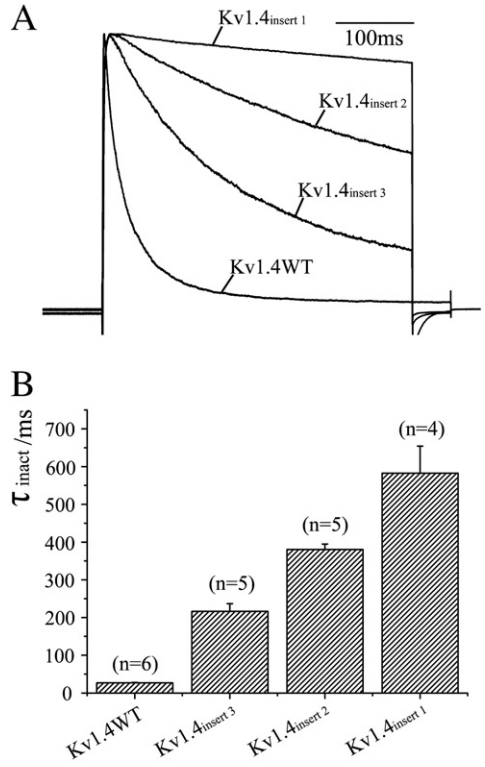

Fig. 9. Effect of inserting negatively charged peptide in the NH_2-terminal inactivation domain. (A) Normalized current traces for Kv1.4WT, $Kv1.4_{insert1}$, $Kv1.4_{insert2}$ and $Kv1.4_{insert3}$ at +70 mV. (B) Comparison of inactivation time constants for Kv1.4WT and the 3 inserting mutants. The number of cells tested is given in the parentheses.

exhibited a too small and positively charged center hole of T1 assembly [27]. Besides the small center hole of T1, the crystal structure of Kv1.2 also exhibited four large side portals formed by the T1–S1 linkers [21]. The side portal is big enough and rich of acidic amino acids, which makes it a good candidate for the position to interact with the positively charged hydrophilic region of inactivation domain through long-distance electrostatic interaction.

In this study, we mutated 4 charged amino acids of inactivation domain and T1–S1 liner to amino acids of opposite polar respectively and obtained the results that both mutants especially $Kv1.4_{R-E}$ slowed the inactivation significantly. The decelerating effect caused by mutating charged amino acids of inactivation domain is consistent with the investigation of Tseng-Crank, who demonstrated that deleting domain I (residues 26–37) greatly attenuated the inactivation rate of inactivation process of Kv1.4 channel [13]. This result is also consistent with the studies in ShB channel, in which deleting the hydrophilic domain of inactivation ball or mutating the positive charges of inactivation ball slowed the inactivation of ShB channel [2]. Our results confirm the roles of charges of both of the two regions in "ball-and-chain" type inactivation of Kv1.4 channel. $Kv1.4_{both}$, of which both the charged inactivation ball and T1–S1 linker were mutated, inactivated more rapidly than $Kv1.4_{R-E}$ of which the mutation was done only on inactivation ball. This result indicates that there exists electrostatic interaction between inactivation domain and T1–S1 linker. Despite the same number of residues mutated, $Kv1.4_{R-E}$ inactivated more slowly than $Kv1.4_{E-R}$, which indicates that the charges on the hydrophilic region of inactivation domain exert a larger effect on the inactivation of Kv1.4 channel than that of T1–S1 linker. We also examined charge screening effect on inactivation of $Kv1.4_{R-E}$ by elevating $[Mg^{2+}]_i$. The more rapid inactivation rate of $Kv1.4_{R-E}$ in 20 mM $[Mg^{2+}]_i$ compared with that in 2 mM $[Mg^{2+}]_i$ indicates the existence of electrostatic repulsion between mutated inactivation domain and T1–S1 linker region in this mutant. Besides forward inactivation rate, the backward (recovery) rate from inactivation was also examined for $Kv1.4_{R-E}$. Contrast to the large difference of inactivation rates, the recovery rate of $Kv1.4_{R-E}$ was not significantly different from that of Kv1.4WT. This result is consistent with the study of Rasmusson, who demonstrated that recovery of Kv1.4 channel is governed by the slow C-type mechanism [28].

To further confirm the electrostatic interactions between inactivation domain and T1–S1 linker region, we subsequently inserted a negatively charged peptide in different positions of inactivation domain of Kv1.4 channel. Residues 19, 39 and 50 were chosen as sites after which the negatively charged peptide was inserted. The secondary structure of amino terminal of Kv1.4 channel is presumed not to be disrupted, because all the inserting sites are in unstructured flexible region according to NMR-derived solution structure of N-terminal of Kv1.4 channel [23]. The significantly decelerated inactivation rate of all the mutants compared with that of Kv1.4WT confirmed the roles of charged amino acids of inactivation domain in the inactivation process of Kv1.4 channel. The extreme amino terminal was presumed to point upward when approaching to its binding site according to our previous study [24], so the mutant with inserting site nearer to the extreme NH_2-terminal end has larger electrostatic repulsion between the inactivation domain and the T1–S1 linker region and thus inactivated more slowly. Solution structure studies on inactivation domain of Kv1.4 channel showed that, different from the compactly folded structure of Kv3.4 channel, the inactivation domain of Kv1.4 channel is more flexible and less ordered [23,29]. The inactivation domain I (ID1, residues 1–38) comprises a flexible NH_2-terminus formed by the first 20 amino acids and a 5-turn α-helix between residues 21 and 38 [23]. The inserting site of $Kv1.4_{insert1}$ is at the COOH-terminal of the flexible domain. So, although the possibility of disruption of ball structure cannot be ruled out, the distinct change in inactivation rate of $Kv1.4_{insert1}$ compared with Kv1.4WT could probably be attributed to the electrostatic interaction between the inserting peptide and T1–S1 linker. According to Wissmann's study, residues 40–50 following ID1 domain constitute a second inactivation domain (ID2), which, as a docking domain, promotes inactivation of Kv1.4 channel by attaching ID1 near the mouth of the channel pore [23]. Although we tend to explain the decelerated inactivation rate of $Kv1.4_{insert3}$ by electrostatic repulsion between the inserted peptide after residues 50 and T1–S1 linker region, it is possible that the inserting mutation near ID2 affects the role of it as a docking domain.

The results in this study have confirmed the role of electrostatic interactions between the inactivation domain and T1–S1 linker on inactivation of Kv1.4 channel. However, $Kv1.4_{R-E}$ mutated on inactivation domain inactivated more slowly than $Kv1.4_{E-R}$ mutated on T1–S1 linker despite the same number of charged amino acids mutated. Obviously, the positive charges of inactivation domain have larger effect on inactivation than negative charges of T1–S1 linker. A probable reason is that there exist other negatively charged regions interacting with inactivation domain through long-distance electrostatic interactions. Ehud's study in ShB had suggested that the S4–S5 loop probably formed part of receptor for the inactivation gate [10]. Because there are not net negative charges in this region of Kv1.4 channel, we do not think it could be a candidate site to interact with inactivation domain of Kv1.4 channel by long distance electrostatic interactions. Besides T1–S1 linkers, there are several net negative charges in the COOH-terminal part of T1 region of Kv1.4, which are not mutated in this study in order to keep the structure of Kv1.4 channel undisturbed. Thus, it is possible that the negative charges of T1–S1 linker combining charges on top surface of T1 assembly interact with positive charges of inactivation domain by long-distance electrostatic interactions which direct the moving of inactivation ball toward its binding site and accelerate the inactivation rate of Kv1.4 channel. Considering that, it is not surprising to obtain the result that $Kv1.4_{E-R}$ mutated on T1–S1 linker inactivated more rapidly than $Kv1.4_{R-E}$ mutated on the inactivation domain. We speculate that the charges on T1 surface may take a larger part in

interacting with inactivation ball compared with T1–S1 linker, for the inactivation rate of $Kv1.4_{R-E}$ is more than two folds of $Kv1.4_{E-R}$. Furthermore, several studies have identified the role of COOH-terminal in inactivation of some channel. For example, the arginines at the COOH-terminus of Kv4 channel have been implicated in the regulation of channel inactivation [30]. Additionally, a COOH-terminal helix of Kv1.4 channel may stabilize the inactivation by wrapping around the T1 surface [31]. The possible role of COOH-terminal effect on channel inactivation may be another reason for the prominent difference of inactivation rates between $Kv1.4_{R-E}$ and $Kv1.4_{E-R}$.

This study demonstrated the electrostatic interaction between positively charged inactivation ball and acidic T1–S1 linker region using mutagenesis method. Combining our previous work, which identified the electrostatic interaction between oppositely charged segment A (residues 83–98) and segment B (residues 123–127) [24], we draw a figure of 3-step inactivation process for Kv1.4 channel (Fig. 10). Firstly, oppositely charged segment A and segment B interact with each other through electrostatic attractions, shortening the distance between inactivation ball and its binding site. Secondly, the inactivation domain passes through the large side portal formed by T1–S1 linkers, with the hydrophobic amino-terminal domain reaching below the intracellular entryway of the channel pore and the positively charged hydrophilic domain lining on the top surface of T1 assembly and/or the rim of T1–S1 linker. Finally, the hydrophobic domain of the inactivation ball enters into the inner pore after it is open. The "sequential-step" model implies two separate steps in inactivation process: first, the approach of the inactivation domain toward the channel pore through long-distance electrostatic interactions (preinactivation) and, second, the binding of inactivation domain to its receptor site through hydrophobic interactions [8]. Our 3-step inactivation process is consistent with the "sequential-step" model except the additional electrostatic interaction between segment A and segment B. Moreover, we confirm the long-distance electrostatic interaction between inactivation ball and T1–S1 linker region.

Wissmann et al. has proposed that the amino terminal of Kv1.4 consists of 2 inactivation domains. Functional analysis suggests that ID1 (residues 1–38) rather than ID2 (residues 40–50) is the pore-occluding domain and ID2 may work as a docking domain which attaches ID1 to the cytoplasmic face of the channel and promotes its rapid access to its receptor site. This model is different from ours in that it presumes the hydrophobic ID2 anchors the inactivation domain (ID1) near the mouth of the pore in preinactivation step, but we emphasize the electrostatic interaction between positively-charged residues of hydrophilic domains of ID1 and T1–S1 linker. However, whether the electrostatic interaction in our model is transient or not remains to be elucidated. It is necessary to estimate the distance between C-terminal of T1 assembly and the inner pore. According to the crystal structure of Kv1.2 channel, T1 domain is about 40 Å in length along the fourfold axis whereas the N terminus of the structured T1 assembly is about 50 Å from the pore [21]. So the distance between the superface of T1 domain and the pore is about 10 Å or more. Adding up to the ~18 Å length of inner pore [32], the separation between the negatively charged T1–S1 linker and the inner cavity of channel pore is about 28 Å. There are 25 amino acids, comprising a flexible N-terminal formed by the first 20 amino acids and a small part of the flowing α-helix structure, preceding the positively-charged region of inactivation ball [23]. So it is possible for the amino terminal of inactivation ball to reach its binding site in the inner cavity of channel pore without dissociation of the positively-charged hydrophilic domain from T1–S1 linker region. Antz et al.'s study showed the NMR structure of inactivation peptides of Kv3.4 and Kv1.4 [29]. In their study, the inactivation peptide of Kv3.4 has a compact structure, and the NH_2-terminus is located in close proximity to the COOH-terminus for the convenience of formation of intramolecular disulphide bond. The structure of inactivation peptide of Kv1.4 in their study is more flexible. Although the N- and C-termini of inactivation peptide of Kv1.4 are not so near to each other as those of Kv3.4, the β-turn in the middle of inactivation peptide may shorten the distance between its N- and C-termini by forming an angle. So the distance between N- and C-termini of ID1 may not be long enough to maintain anchoring of the positively charged segment to the T1–S1 region while the hydrophobic ball entering the mouth of the channel. In other words, the binding of positively charged segment of ID1 to T1–S1 linker region may be transient. Nevertheless, the inactivation process in actual biological systems is more complicated. In the absence of high resolution crystallographic data on the inactivated channel/peptide complex, any predictions from model systems should be taken as a reasonable guess about the behavior that real molecules are likely to exhibit.

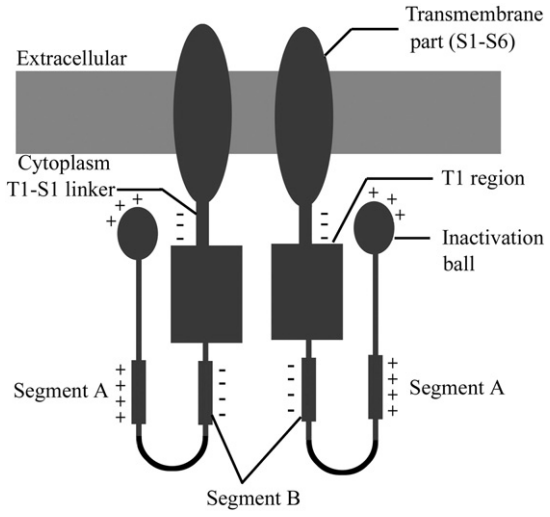

Fig. 10. Schematic representation of the electrostatic interactions in Kv1.4 channel. The positively and negatively charged regions have been indicated. Segment A (residues 83–98) interacts with segment B (residues 123–137) through electrostatic attraction, which has been demonstrated in our previous article. Long-distance electrostatic interaction between positively charged inactivation ball and negatively charged T1–S1 linker facilitates the inactivation of Kv1.4 channel.

Acknowledgements

This work was supported by grants from the National Natural Science Foundation of China (Grant Nos. 30730039, 30970982, 31171059). We are grateful to Professor. Z. Qi for his instruction in patch clamp recording technology and to Drs. R.K. Wu (School of Foreign Studies of our university) for his help with the language polishing.

References

[1] B. Hille, Ion Channels of Excitable Membranes, third ed. Sinauer Associates, Sunderland, MA, 2001.
[2] T. Hoshi, W.N. Zagotta, R.W. Aldrich, Biophysical and molecular mechanisms of *Shaker* potassium channel inactivation, Science 250 (1990) 533–538.
[3] W.N. Zagotta, T. Hoshi, R.W. Aldrich, Restoration of inactivation in mutants of *Shaker* potassium channels by a peptide derived from ShB, Science 250 (1990) 568–571.
[4] C.M. Armstrong, F. Bezanilla, Currents related to movement of the gating particles of the sodium channels, Nature 242 (1973) 459–461.
[5] C.M. Armstrong, F. Bezanilla, Inactivation of the sodium channel II, J. Gen. Physiol. 70 (1977) 567–590.
[6] F. Bezanilla, C.M. Armstrong, Inactivation of the sodium channel I, J. Gen. Physiol. 70 (1977) 549–566.
[7] J.A. Encinar, A.M. Fernández, E. Gil-Martín, F. Gavilanes, J.P. Albar, J.A. Ferragut, J.M. González-Ros, Inactivating peptide of the *Shaker* B potassium channel: conformational preferences inferred from studies on simple model systems, Biochem. J. 331 (1998) 497–504.
[8] M. Zhou, J.H. Morais-Cabral, S. Mann, R. MacKinnon, Potassium channel receptor site for the inactivation gate and quaternary amine inhibitors, Nature 411 (2001) 657–661.
[9] J.A. Encinar, A.M. Fernández, J.A. Poveda, M.L. Molina, J.P. Albar, F. Gavilanes, J.M. Gonzalez-Ros, Probing the channel-bound *Shaker* B inactivating peptide by

stereoisomeric substitution at a strategic tyrosine residue, Biochemistry 42 (2003) 8879–8884.
[10] E.Y. Isacoff, Y.N. Jan, L.Y. Jan, Putative receptor for the cytoplasmic inactivation gate in the *Shaker* K^+ channel, Nature 353 (1991) 86–90.
[11] R.D. Murrell-Lagnado, R.W. Aldrich, Energetics of *Shaker* K^+ channels block by inactivation peptides, J. Gen. Physiol. 102 (1993) 977–1003.
[12] J.A. Encinar, A.M. Fernandez, F. Gavilanes, J.P. Albar, J.A. Ferragut, J.M. Gonzalez-Ros, Interaction between ion channel-inactivating peptides and anionic phospholipid vesicles as model targets, Biophys. J. 71 (1996) 1313–1323.
[13] J. Tseng-Crank, J.A. Yao, M.F. Berman, G.N. Tseng, Functional role of the NH_2-terminal cytoplasmic domain of a mammalian A-type K channel, J. Gen. Physiol. 102 (1993) 1057–1083.
[14] Y. Hashimoto, K. Nunoki, H. Kudo, K. Ishii, N. Taira, T. Yanagisawa, Changes in the inactivation of rat Kv1.4 K^+ channels induced by varying the number of inactivation particles, J. Biol. Chem. 275 (2000) 9358–9362.
[15] F.R. Fernandez, E. Morales, A.J. Rashid, R.J. Dunn, R.W. Turner, Inactivation of Kv3.3 potassium channels in heterologous expression systems, J. Biol. Chem. 278 (2003) 40890–40898.
[16] G.J. Stephens, B. Robertson, Inactivation of the cloned potassium channel mouse Kv1.1 by the human Kv3.4 'ball' peptide and its chemical modification, J. Physiol. 484 (1995) 1–13.
[17] R. Bähring, L.M. Boland, A. Varghese, M. Gebauer, O. Pongs, Kinetic analysis of open- and closed-state inactivation transitions in human Kv4.2 A-type potassium channels, J. Physiol. 535 (2001) 65–81.
[18] T.E. Lee, L.H. Philipson, D.J. Nelson, N-type Inactivation in the Mammalian *Shaker* K^+ Channel Kv1.4, J. Membr. Biol. 151 (1996) 225–235.
[19] H.T. Kurata, Z. Wang, D. Fedida, NH_2-terminal inactivation peptide binding to C-type-inactivated Kv channels, J. Gen. Physiol. 123 (2004) 505–520.
[20] R.L. Rasmusson, S. Wang, R.C. Castellino, M.J. Morales, H.C. Strauss, The beta subunit, Kv beta 1.2, acts as a rapid open channel blocker of NH_2-terminal deleted Kv1.4 alpha-subunits, Adv. Exp. Med. Biol. 430 (1997) 29–37.
[21] S.B. Long, E.B. Campbell, R. Mackinnon, Crystal structure of a mammalian voltage-dependent *Shaker* family K^+ channel, Science 309 (2005) 897–903.
[22] S.B. Long, X. Tao, E.B. Campbell, R. MacKinnon, Atomic structure of a voltage-dependent K^+ channel in a lipid membrane-like environment, Nature 450 (2007) 376–382.
[23] R. Wissmann, W. Bildl, D. Oliver, M. Beyermann, H.R. Kalbitzer, D. Bentrop, B. Fakler, Solution structure and function of the "tandem inactivation domain" of the neuronal a-type potassium channel Kv1.4, J. Biol. Chem. 278 (2003) 16142–16150.
[24] Z. Fan, L.J. Bi, G. Jin, Z. Qi, Electrostatic interaction in the NH_2-terminus accelerates inactivation of the Kv1.4 channel, Biochim. Biophys. Acta 1798 (2010) 2076–2083.
[25] R.D. Murrell-Lagnado, R.W. Aldrich, Interactions of amino terminal domains of *Shaker* K channels with a pore blocking site studied with synthetic peptides, J. Gen. Physiol. 102 (1993) 949–975.
[26] S. Kondoh, K. Ishii, Y. Nakamura, N. Taira, A mammalian transient type K^+ channel, rat Kv1.4, has two potential domains that could produce rapid inactivation, J. Biol. Chem. 272 (1997) 19333–19338.
[27] A. Kreusch, P.J. Pfaffinger, C.F. Stevens, S. Choe, Crystal structure of the tetramerization domain of the *Shaker* potassium channel, Nature 392 (1998) 945–948.
[28] R.L. Rasmusson, M.J. Morales, R.C. Castellino, Y. Zhang, D.L. Campbell, H.C. Strauss, C-type inactivation controls recovery in a fast inactivating cardiac K^+ channel (Kv1.4) expressed in Xenopus oocytes, J. Physiol. 489 (1995) 709–721.
[29] C. Antz, M. Geyer, B. Fakler, M.K. Schott, H.R. Guy, R. Frank, J.P. Ruppersberg, H.R. Kalbitzer, NMR structure of inactivation gates from mammalian voltage-dependent potassium channels, Nature 385 (1997) 272–275.
[30] N. Hatano, S. Ohya, K. Muraki, R.B. Clark, W.R. Giles, Y. Imaizumi, Two arginines in the cytoplasmic C-terminal domain are essential for voltage-dependent regulation of A-type K^+ current in the Kv4 channel subfamily, J. Biol. Chem. 279 (2004) 5450–5459.
[31] K. Sankaranarayanan, A. Varshney, M.K. Mathew, N type rapid inactivation in human Kv1.4 channels: functional role of a putative C-terminal helix, Mol. Membr. Biol. 22 (2005) 389–400.
[32] D.A. Doyle, J. Morais Cabral, R.A. Pfuetzner, A. Kuo, J.M. Gulbis, S.L. Cohen, B.T. Chait, R. MacKinnon, The structure of the potassium channel: molecular basis of K^+ conduction and selectivity, Science 280 (1998) 69–77.